

Methodology for modelling a combined DPF and SCR catalyst with the porous medium approach in CFD

Benjamin, S.F. and Roberts, C.A.

Published version deposited in CURVE November 2014

Original citation & hyperlink:

Benjamin, S.F. and Roberts, C.A. (2014) Methodology for modelling a combined DPF and SCR catalyst with the porous medium approach in CFD. SAE International Journal of Engines, volume 7 (4): 1997-2011.

<http://dx.doi.org/10.4271/2014-01-2819>

Publisher statement: Copyright © 2014 SAE International. This paper is posted on this site with permission from SAE International and is for viewing only. It may not be stored on any additional repositories or retrieval systems. Further use or distribution is not permitted without permission from SAE.

Copyright © and Moral Rights are retained by the author(s) and/ or other copyright owners. A copy can be downloaded for personal non-commercial research or study, without prior permission or charge. This item cannot be reproduced or quoted extensively from without first obtaining permission in writing from the copyright holder(s). The content must not be changed in any way or sold commercially in any format or medium without the formal permission of the copyright holders.

CURVE is the Institutional Repository for Coventry University

<http://curve.coventry.ac.uk/open>

Methodology for Modelling a Combined DPF and SCR Catalyst with the Porous Medium Approach in CFD

S. F. Benjamin and C. A. Roberts
Coventry Univ.

ABSTRACT

In an attempt to reduce particulate and NO_x emissions from Diesel exhaust, the combined DPF and SCR filter is now frequently chosen as the preferred catalyst. When this device functions effectively it saves valuable packaging space in a passenger vehicle. As part of its development, modelling of its emissions performance is essential. Single channel modelling would seem to be the obvious choice for an SCR filter because of its complex internal geometry. This, however, can be computationally demanding if modelling the full monolith. For a normal flow-through catalyst monolith the porous medium approach is an attractive alternative as it accounts for non-uniform inlet conditions without the need to model every channel. This paper attempts to model an SCR filter by applying the porous medium approach. The model is essentially 1D but as with all porous medium models, can very easily be applied to 3D cases once developed and validated. The model is described in full in this paper and values for all the key parameters are presented. The filter is assumed to collect soot in the inlet channels, but only the outlet channels are coated with SCR washcoat, as in the most recent devices. This aims to avoid back diffusion of NO₂ that promotes soot and NO_x reactions. But it is necessary to modify the pressure loss expression term to account for the smaller size of the washcoated outlet channel. The SCR model integrated into the CFD coding is simple and based on a scheme available in the literature. This includes the standard and fast SCR reactions and ammonia adsorption and desorption. NO and ammonia oxidation are also included and are important during the high temperature regeneration phase. The detail of the flow at the channel scale is not modelled but the species can be modelled at the channel scale for the monolith by application of source terms in the species transport equation. The source terms are evaluated in user subroutines in commercial CFD software. The species levels of NO, NO₂ and NH₃ in the flow coming through the filter wall, in the pores in the wall and in the flow in the downstream channel are all modelled as a function of distance along the brick. The simplifying assumptions on which this model is based are stated in this paper. The model produces plausible output when run as a demonstration case for a 1050 s soot storage period at 550 K, followed by a 150 s regeneration period at 900 K, and then for a further soot storage period at 550 K. The simulations are in qualitative agreement with the expected performance of a combined DPF and SCR in a real Diesel exhaust. An attempt has been made to apply the model to a real case based on data available in the literature so that its output can be validated.

CITATION: Benjamin, S. and Roberts, C., "Methodology for Modelling a Combined DPF and SCR Catalyst with the Porous Medium Approach in CFD," *SAE Int. J. Engines* 7(4):2014, doi:10.4271/2014-01-2819.

INTRODUCTION

Passenger cars with Diesel engines are now in common usage because of good fuel efficiency and relatively low emissions of CO and hydrocarbons. Particulate emissions and NO_x, however, remain challenging as the emissions regulations become ever more restrictive. The DPF is established as the method of choice for the removal of particulates and SCR catalysts have been shown to be effective in removing NO_x. Recently, the DPF and the SCR have been combined into a single unit, sometimes called an SCR filter (SCR filter) or WFSR (wall flow SCR). This combined device occupies less space in the exhaust system than a separate filter and SCR catalyst for aftertreatment. As with all aftertreatment devices, it is desirable that the emissions performance of the device can be modelled.

The geometry of the DPF, the catalysed DPF and the combined SCR/DPF is by its nature more complex to model than the flow-through multi-channel catalyst substrate.

There are at least three separate research teams working on the issue of SCR filter modelling who have published widely. Haralampous et al. [1, 2] began some years ago by modelling catalysed DPFs; they have published extensively on catalysed DPFs where the catalyst was intended to promote the regeneration, which occurred by oxidation of soot with either oxygen or NO₂. Their modelling approach was mathematically rigorous with the full model description presented as a set of equations in their papers. They later moved on to modelling

combined DPF-SCR devices [3, 4]. In these later papers they have utilised the specialised software package Axisuite to solve the equations.

York et al. also investigated catalysed DPFs initially [5, 6]. But by 2012 [7] this team had also turned their attention to the SCR. They attempted to model the performance of an SCR and also to validate their model. Unfortunately, their model is not readily applicable by other users because some details, including kinetic constants, are not presented. Park et al. [8] have also published a paper, which is specifically a modelling study of SCR-DPF devices. They mention the mass transfer in the inlet and outlet channels of the DPF being influenced by suction at the wall in the inlet channels and blowing at the wall in the outlet channels, which is a detail that is not commented upon by most authors. They have published again on this topic [9] and have investigated mass transfer differences between flow-through and wall-flow devices. In this later paper they suggest that wall-flow devices are less efficient in converting NO_x than flow-through devices, but their paper is not focused on developments to the model itself.

In an SCR, the flow passing through the porous walls of the filter into adjacent channels is orthogonal to the main flow direction through the substrate as a whole. This implies that modelling the individual channels may be necessary to describe the detail of the processes within the catalysed filter when developing a CFD model. A single channel modelling approach will provide a complete description of a situation where the main flow direction is aligned with the channels as in a normal multi-channel catalyst, or if several channels are modelled, it can follow the flow through the wall from channel to channel in a DPF. For a normal flow-through catalyst substrate there is a computational option, which is modelling using the porous medium approach. This considers the whole substrate as an analogous porous medium and has the advantage of computational efficiency. The mesh size is often coarser than the cross sectional dimensions of the channels and so a smaller number of computational cells is required for a large 3D model. In 2007, an attempt was made by the authors to model a DPF using the porous medium approach. This was an evaluation exercise and was computationally successful, although the model was not fully validated [10]. For the DPF or the newer combined DPF/SCR it may initially appear counter-intuitive to model the device using the porous medium approach. The advantages of the porous medium approach, however, make the attempt to model the combined DPF and SCR in this way worthwhile. The detail of the flow at the channel scale is not modelled by this approach but the species can be modelled at the channel scale for the monolith by application of source terms in the species transport equations. The attempt reported in this paper demonstrates that modelling in this way is indeed feasible for assessing conversion efficiency. The SCR kinetic model integrated into this model is based on a scheme published by Olsson et al. [11]. Soot oxidation is included as in an earlier paper by the authors [10] and a reaction rate for the reaction between soot and NO₂ can also be included; Ahmadinejad et al. [12] and

Zouaoui et al. [13] have both investigated the kinetics of the reaction between soot and NO₂. The model as presented in this paper is essentially a demonstration model but it has been applied to real cases and compared with data presented in the literature [14]. The model as developed and described here is essentially 1D but the advantage of the porous medium approach is that, once validated, it can very easily be adapted and extended to 3D cases.

Park et al. [8] present a useful comparison between the time scales for convection and diffusion in a combined DPF-SCR device. They suggest that convection along the channel and diffusion to the filter wall have the same time scale in the inlet channel but that diffusion along the inlet channel is 4 orders of magnitude slower and hence negligible. This is presumably also true in the outlet channel. When the flow passes through the filter wall, diffusion in the flow direction and diffusion to the catalyst surface are an order of magnitude faster than convection through the wall. Other authors have made different assumptions, and most do not comment on any diffusion occurring in the direction of the net convective flow through the wall. Ahmadinejad et al. [12] assume that reactants reach the soot by convection only and so did not consider diffusion. Watling et al. [7] state that diffusion to the surfaces from convective flow both through the wall and along the channels should be considered in an SCR model. They apply mass transfer terms to account for this. This diffusion issue does present a challenge to the application of the porous medium approach to an SCR as any gradient in concentration through the wall must be assumed to be linear. Nevertheless a transfer coefficient can be applied to the bulk flow through the wall to allow for lateral diffusion to the sites within the wall. This is discussed later in this paper.

The aim of this work is to demonstrate that the combined DPF/SCR or SCR can be modelled as a homogeneous entity using the porous medium approach. The aim is to develop a model that will circumvent the need to use representative single channels when modelling cases with a complex 3D flow field. The time advantage achieved when using smaller numbers of computational cells with the porous medium approach is considerable. This report gives full details of the model, which is developed in Star-CD Version 4.14. The source terms, which are discussed in detail in this paper, have been coded into user subroutines of the CFD code. This is a novel approach to modelling this device which has flow passing through the filter walls in directions orthogonal to the main flow direction. The model developed in this paper is 1D but is readily transferable to 3D geometries.

ASSUMPTIONS MADE IN FORMULATING THE POROUS MEDIUM DPF-SCR MODEL

When modelling any multichannel catalyst substrate as an analogous porous medium in Star-CD, the gas phase and solid pore phase species concentrations are both properties of the porous fluid cells. The DPF-SCR or SCR that is modelled in this

paper has a washcoated SCR layer only in the outlet channel. A schematic diagram is shown in [Figure 1](#). When modelling an SCRf, the inlet species concentration ($\rho_{in}C_{in}$) and mass fraction C_{in} are known. There are four other locations where the species mass fractions are solved for and are of particular interest. Those four locations are: in the porous wall after the soot layer, in the gas filled pore within the SCR washcoat layer, in the gas as it flows from the SCR washcoat layer into the outlet channel, and in the gas flow along the outlet channel.

The general conservation equation for chemical species is the transport equation. [Equation \(1\)](#) is the full 3D version of this equation.

$$\frac{\partial(\rho C)}{\partial t} + \nabla \cdot (\rho UC) - \nabla \cdot \left[\frac{\mu_t}{\sigma_s} + \rho D \right] \nabla C = \dots$$

$$= Source \text{ kg m}^{-3} \text{ s}^{-1}$$

(1)

The three terms of this equation on the left are the transient term, the convective term and the diffusion flux term. The source term on the right hand side is only applicable within the porous medium computational cells when the porous medium approach is implemented, for example in a multichannel catalyst substrate. In that case the source term describes the net effect of diffusion of species between the gas stream and the washcoat pores at the channel wall as a mass transfer process. So, in effect, the source term replaces the diffusion flux term in the direction normal to the flow direction. This is achieved by using a mass transfer coefficient. The diffusion flux in the flow direction in a porous medium is usually assumed to be negligibly small compared with the convective flux. To model an SCRf, for the purposes of this paper, it is possible to consider a hypothetical channel pair and solve [eq. \(1\)](#) in the y and z directions only. [Equation \(1\)](#) is written in its 1D form as [eq. \(2\)](#), for axial flow along the analogous porous medium, with the diffusion flux term suppressed, which is achieved within Star-CD by the choice of values for σ_s and D.

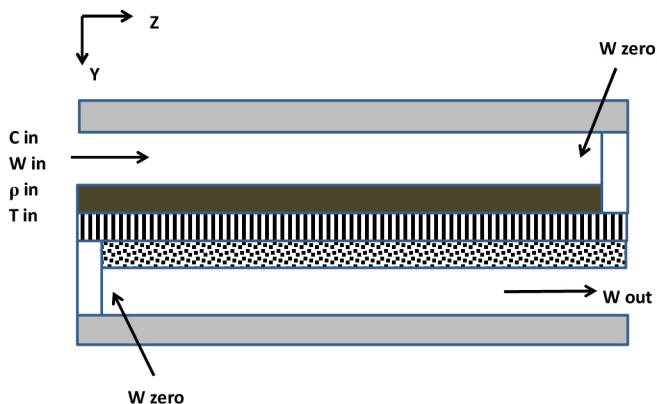


Figure 1. Schematic diagram of a combined SCR/DPF or SCRf or WFSR showing the detail of one wall between a hypothetical channel pair. Soot layer is black; porous wall is shown striped; SCR washcoat layer is dotted black. Blocked channel ends are shown in white. W is velocity in z direction.

$$\frac{\partial(\varepsilon \rho C)}{\partial t} + \frac{\partial(\varepsilon \rho WC)}{\partial z} = Source \text{ kg m}^{-3} \text{ s}^{-1}$$

(2)

In an SCRf the pores where the reactions will take place are accessed by the flow as it passes through the tortuous passages in the SCR washcoated layer. In that layer, where the net flow direction is normal to the SCRf channels, the magnitudes of mass transfer by convection and by diffusion are closer in magnitude, because the net flow velocity through the wall is low. The second order diffusion term in the y direction may therefore not be negligible in some cases but it has been neglected in this model as a first approximation for the purposes of demonstration of the model methodology. For flow through the porous layer in the net y direction, the general equation, [eq. \(1\)](#), is rewritten as [eq. \(3\)](#). Transfer to the pores in the washcoat, which is a lateral diffusion process within the porous wall, is dealt with by the source term, using a mass transfer coefficient that is referenced in [Appendix A](#).

$$\frac{\partial(\varepsilon \rho C)}{\partial t} + \frac{\partial(\varepsilon \rho VC)}{\partial y} = Source \text{ kg m}^{-3} \text{ s}^{-1}$$

(3)

The model described here aims to simulate the combined DPF/SCR as a homogeneous entity using the porous medium approach. In order to achieve this and to model the detail of the processes in these dual-channel devices, numerous assumptions are necessary, which are listed here. These assumptions in turn require adaptations to be made to the equations solved within the CFD code Star-CD.

- [1]. It is assumed that there is no mass transfer occurring between adjacent channel pairs.
- [2]. [Table B1](#) in Appendix B lists the species defined in the model. The gas concentrations (ρC_g) are those in the inlet channel. The concentrations (ρC_{ps}) are post the soot layer, which means the concentrations in the wall after the soot reactions have occurred. The pore concentrations (ρC_{pore}) are the local concentrations inside the SCR washcoat layer. The concentrations (ρC_w) as the gas leaves the wall are the gas phase concentrations in the flow that passes through and out from the wall in the y direction at each specified z location. The ammonia storage in the wall, characterised by parameter θ , is similarly a function of z. The outlet channel concentrations (ρC_{out}) are the gas phase concentrations in the flow, which in the real SCRf convects in the z direction along the outlet channel towards the exit.
- [3]. The simulation assigns a convective velocity in the z direction to each computational cell when the combined DPF/SCR is considered as a whole and modelled as an equivalent porous medium. This is not the true convective velocity in either the upstream or the downstream channel. It is an effective velocity for a hypothetical channel pair. Detailed modelling of the upstream channel is circumvented since the function of this channel is only soot filtration as modelled previously for a simple non-catalysed DPF [10].

- [4]. In the outlet channel downstream of the porous wall the convective velocity varies from zero at $z = 0$ up to the convective velocity corresponding to the full mass flow rate at the exit from the channel of the SCR. The assumption is made that the mass flow distributes itself uniformly when it enters the wall from the inlet channel. This necessitates coding strategies in the user subroutine for the species source terms to force the CFD solver to calculate values that represent the true mass fractions, and hence concentrations, in the downstream channel.
- [5]. The nominal wetted area A_v (m^2/m^3 substrate) is based on all the channels of an SCR. The filtration area is approximately half of this because soot accumulates only in the inlet channels. When only the outlet channels are coated with washcoat and SCR catalyst, then the wetted area in the outlet channels is smaller than the filtration area offered by the inlet channels. This is because the washcoat layer thickness is accounted for in the evaluation of the wetted SCR surface area in the outlet channels.
- [6]. The parameter V_w is a measure of the pore volume in the SCR washcoat layer per m^3 of bulk substrate and is dependent upon SCR geometry, the SCR washcoat properties and its loading. An estimated value for an SCR is about $0.05 m^3$ pore volume / m^3 substrate, assuming the washcoat porosity is in the range 50 - 60 %.
- [7]. The soot layer thickness in the inlet channel is negligible initially but the wall is assumed already permeated with soot so that soot accumulates on the surface as a cake. The filter is 100 % efficient in removing soot from the flow.
- [8]. There is no significant diffusion or reaction of species in the inlet channel so that the concentrations of the incoming species are uniform along the inlet channel. Change in the concentration of NO , O_2 and NO_2 by reaction with soot occurs as the flow passes through the soot layer. The reaction rates for the soot reactions are calculated using the gas phase NO_2 and O_2 concentrations.
- [9]. The SCR reactions take place in the pores in the SCR washcoat layer. There is mass transfer between the flow through the washcoat layer and the pores in the layer; the pore phase concentrations are used to calculate the reaction rates for the SCR reactions. The mass transfer coefficient for transfer between the flow through the SCR washcoat layer and the pores is discussed in [Appendix A](#) of this paper.
- [10]. The concentration of the species NO , NO_2 and NH_3 in the flow that passes into the downstream channel is controlled by reactions that have already occurred as the flow has passed through the soot layer, and through the catalytically active washcoat layer on the wall in the outlet channel.
- [11]. In the outlet channel there is convection in the z direction, but negligible diffusion in the z direction. There can be exchange by diffusion, however, in the y direction between the outlet channel flow and the relatively slow flow through the SCR washcoat layer. This is accounted

for in the model by a mass transfer source term. The mass transfer coefficient is calculated in the normal way in the demonstration model reported here. The wall flow velocity is very low and so the transfer coefficients will be a fair approximation to the real situation. But Hwang et al. [15] consider the effect of suction (which occurs in the inlet channel) and blowing (which occurs in the outlet channel) on wall heat transfer; and there will be a similar effect on mass transfer. The model may need to be modified to account for this at a later stage of its development.

- [12]. If both the inlet channels and outlet channels are coated in SCR washcoat, the soot layer forms directly adjacent to an SCR washcoat layer. There can be back-diffusion of species from the SCR washcoat layer to the soot layer. This back diffusion is particularly significant when NO_2 is present [1]. This is because NO_2 interferes with the soot oxidation during the regeneration. This back diffusion is not currently accounted for in the model described in this paper. The geometry on which this model is based is different because the filter wall separates the SCR layer from the soot cake layer, which is where most of the soot resides.

FORMULATION OF SOURCE TERMS FOR COMBINED DPF-SCR MODEL

The general forms of the transport equation were given in [eqs. \(1\), \(2\), \(3\)](#). Applying the porous medium approach in CFD requires that diffusion is suppressed in the porous medium; but where there is diffusion in the porous medium, which must be accounted for in the model, this is achieved with source terms. In order to account for all of the assumptions discussed in the previous section, the equations and their source terms will take various forms, which are discussed in detail in this section.

The modelling of the two soot species in [Table B1](#) of Appendix B is based on the non-catalysed DPF model previously developed [10]. The contents of the soot cake layer increases from approximately zero to a value that is very large when expressed as a mass fraction of the fluid (gas). In order to solve the transport equation in the CFD model, a multiplier (10^4) is introduced so that [true mass fraction $\times 10^{-4}$] is solved for in the case of this scalar. For the rest of the defined species the mass fraction is solved for, and the species are dealt with as now described.

NO, NO₂, O₂ and NH₃ Concentrations in the Inlet Channel and the Bulk Gas Phase

[Equation \(4\)](#) describes the conservation of gas species for a hypothetical channel pair assuming that there is no mass transfer or gas phase reaction occurring as the species travel from the inlet to the outlet of the monolith. Hence the source term is zero in [eq. \(4\)](#), as indicated in [Table B1](#) in Appendix B. The concentration ($\rho_{air} C_g$) can be described as the bulk species concentration in the whole substrate and will remain constant at the inlet concentration if density is unchanged. The density ρ_{air} approximates the exhaust stream density.

$$\frac{\partial(\rho_{air}W_s C_g)}{\partial z} + \frac{\partial(\varepsilon\rho_{air}C_g)}{\partial t} = 0 \quad (4)$$

Note that W_s is the superficial velocity in the z direction for the bulk porous medium, not the inlet or outlet channel velocity. The porosity of the SCRf is the void fraction ε , so that

$$\rho_{air}W_s = \varepsilon\rho_{air}W$$

In eq. (4) the diffusion flux term has been suppressed in the porous medium, but normal values for the diffusion coefficients do apply, however, in the fluid. Values for diffusion coefficients are shown in Table B1. A small mesh has been used for model development, see Figure 2, and the inlet and outlet fluid ducts are shown in blue. In the fluid ducts, the normal RANS equations are solved. The demonstration model presented here is a simple 1D case. In more complex and 3D models there will be a temporal and spatial distribution of inlet velocity and species concentration at the front face of the SCRf. The bulk concentration will therefore change as a consequence of both varying inlet conditions and heat transfer in the monolith.

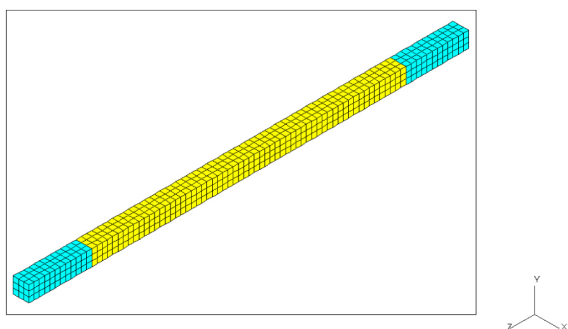


Figure 2. The computational mesh for the combined DPF/SCR or SCRf model with 756 cells each 2.5 mm × 2.5 mm × 2.5 mm; Inlet duct from z = 0 to z = 30 mm (12 cells); Porous medium between z = 30 mm and z = 180 mm (60 cells); Outlet duct from z = 180 mm to z = 210 mm (12 cells).

NO, NO₂, and O₂ Concentrations in the Wall After Reactions with Soot

The flow passes through the soot cake layer in the y direction. The convective term is not included on the left hand side of eq. (5) but is accounted for in the source term. The flow enters the soot layer with concentration ($\rho_{air}C_g$) and leaves with concentration ($\rho_{air}C_{ps}$). The significance of this term is discussed further in relation to eqs. (6), (7), (8). Equation (5) also has diffusion suppressed so that it cannot occur in the z direction in the porous medium.

$$\frac{\partial(\varepsilon\rho_{air}C_{ps})}{\partial t} = \frac{M'(C_g - C_{ps})}{V_{sub}} + \sum SRR \quad kg \ s^{-1}m^{-3} \ reactor \quad (5)$$

The rates for the soot reactions are calculated with gas phase concentrations of NO, NO₂ and O₂.

The quantity M' is the total mass flow rate in kg/s that passes through the DPF/SCR. The quantity V_{sub} is the volume of whole substrate that filters and converts the species in the mass flow. Hence, a value for the mass flow rate in kg/s/m³ substrate is derived in eq. (6). This value applies to the bulk flow through the substrate in the z direction but also to bulk flow through the wall in the y direction, as demonstrated by eqs. (6), (7), (8). Note that $[V_{sub}/L]$ m² is the superficial cross-sectional area of the equivalent continuum through which all the mass flows in the z direction, and A_{filt} (m²/m³) is the wall filtration area per unit volume through which all the flow passes in the y direction.

For the net flow through the porous medium in the z direction with velocity W_s

$$\frac{M'}{V_{sub}} = \frac{W_s\rho_{air}}{L} \quad kg \ s^{-1}m^{-3} \ substrate \quad (6)$$

Also, for flow through the wall in the y direction with superficial velocity V_{wall}

$$M' = V_{wall}\rho_{air}[V_{sub}A_{filt}] \quad kg \ s^{-1}$$

From eq. (7)

(7)

From eq. (7)

$$\frac{M'}{V_{sub}} = V_{wall}\rho_{air}A_{filt} \quad kg \ s^{-1}m^{-3} \ substrate \quad (8)$$

Thus the local value for mass flow rate per unit volume can be found by using the local values of W_s and ρ_{air} in the CFD model, which are temperature dependent, but dividing by the full length of the substrate in the z direction as in eq. (6). Equations (6), (7), (8) show that the net bulk flow into a computational cell (kg/s/m³) is the same for both channel-pair and through-the-wall modelling. This is also applied in the next section.

NO, NO₂, NH₃ and O₂ Concentrations in the Flow Leaving the SCR Wall Layer

For the concentrations in the flow that has passed through the wall, the convective term in the z direction is not included. Equation (9) also has diffusion suppressed so that it cannot occur in the z direction in the porous medium. Three separate terms make up the source term in eq. (9).

$$V_w \frac{\partial(\rho_{air}C_w)}{\partial t} \quad kg \ s^{-1}m^{-3} \ reactor = \left\{ M' \frac{(C_{ps} - C_w)}{V_{sub}} + \dots \right. \\ \left. + K_{mi}\rho_{air}(A_v/2)(C_{out} - C_w) + K_{pore}S_A\rho_{air}(C_{pore} - C_w) \right\} \quad (9)$$

V_w is the fraction of the overall substrate volume that is occupied by pores (tortuous capillaries) in the SCR washcoat. The flow through the wall must pass through these and the SCR reactions can only occur at the catalytically active surfaces inside these pores or capillaries. The first term on the right hand side of eq. (9) accounts for the fact that all the mass flow passes through the active SCR washcoat layer in the net y direction along its the tortuous path. This introduces the species into the volume V_w with concentration ($\rho_{air}C_{ps}$) but when the flow leaves the wall it has concentration ($\rho_{air}C_w$). Within the coding, application of eqs. (6), (7), (8) provides a value for M'/V_{sub} . The mass transfer between the flow through the wall and the active sites in the pores is dealt with by the final term of eq. (9). Estimation of a value for K_{pore} is made using the information in Appendix A of this paper. The middle term on the right hand side of eq. (9) is a mass transfer term that models diffusion in the y direction in the outlet channel and accounts for the possibility of a small amount of species transfer from the outlet channel concentration back to the concentration in the flow that emerges from the wall.

Equation (9) is re-expressed as eq. (10) for solution within Star-CD.

$$\begin{aligned} \varepsilon \frac{\partial(\rho_{air}C_w)}{\partial t} \text{ kg s}^{-1}\text{m}^{-3} \text{ reactor} = & \left\{ M' \frac{(C_{ps} - C_w)}{V_{sub}} + \dots \right. \\ & + K_{mi}\rho_{air} \left(A_v/2 \right) (C_{out} - C_w) + \dots \\ & \left. + K_{pore}S_A\rho_{air}(C_{pore} - C_w) \right\} \varepsilon / V_w \end{aligned} \quad (10)$$

NO, NO₂, NH₃ and O₂ in the Pores in the SCR Layer on the Wall

The rates of change of the concentrations in the pores, see Table B1, in units of kg/s/m³ reactor are described by eq. (11):

$$V_w \frac{\partial(\rho_{air}C_{pore})}{\partial t} = \{ K_{pore}\rho_{air}S_A(C_w - C_{pore}) + M_iR_i \} \quad (11)$$

Equation (11) is rewritten as eq. (12) for solution within Star-CD.

$$\varepsilon \frac{\partial(\rho_{air}C_{pore})}{\partial t} = \left\{ K_{pore}\rho_{air}S_A(C_w - C_{pore}) + M_iR_i \right\} \varepsilon / V_w \quad (12)$$

The second term on the right hand side of eq. (12) accounts for the reactions which consume or produce species in the wall and provide a sink or source respectively. The reaction rates are calculated using the local gas phase concentrations inside the pores. The mass transfer between the flow through the wall and the pores in the washcoat layer is quantified by use of the mass transfer coefficient discussed in Appendix A.

Ammonia storage parameter, θ

For the ammonia storage parameter, θ in Table B1, eq. (13) applies, where R_{ads} is the ammonia adsorption rate, R_{des} is the desorption rate and R_{rx} is the reaction rate.

$$\Omega \frac{\partial\theta}{\partial t} = R_{ads} - R_{des} - R_{rx} \text{ mol s}^{-1}\text{m}^{-3} \text{ reactor} \quad (13)$$

Equation (13) is re-expressed as eq. (14) for solution within Star-CD, with units kg s⁻¹ m⁻³.

$$\varepsilon\rho_{air} \frac{\partial\theta}{\partial t} = \frac{\varepsilon\rho_{air}}{\Omega} (R_{ads} - R_{des} - R_{rx}) \quad (14)$$

In eq. (14) the source term utilises the pore concentrations to calculate the rates. The capacity parameter Ω mol/m³ reactor will have a value appropriate for the combined SCR/DPF, which will depend upon SCR catalyst loading and the assumption that only the outlet channels are SCR washcoated.

NO, NO₂, NH₃ and O₂ in the SCRF Outlet Channel

For the outlet channel, when solving for species mass fractions, and hence concentrations, there is an additional issue to consider. Equation (15) is a version of the transport equation without the convection term and without the diffusion term but with convection accounted for by means of an extra source term, as noted in Table B1. Diffusion is suppressed in the porous medium because it is assumed to be not significant in the flow in the z direction when compared with convection. Suppressed values for the diffusion coefficients also apply in the fluid in the inlet and outlet duct regions, so the outlet mass fractions and concentrations are available only in the porous medium in the CFD model, despite the fact that there is convection in the real case. Any back diffusion of species in the y direction in the outlet channel is dealt with by the first source term on the right hand side of eq. (15), which describes mass transfer between the concentration in the flow in the outlet channel and the flow emerging from the wall. This generally has only a very small effect but is included.

$$\begin{aligned} \varepsilon \frac{\partial(\rho_{air}C_{out})}{\partial t} \text{ kg s}^{-1}\text{m}^{-3} \text{ reactor} = & \dots \\ = & -K_{mi}\rho_{air}(A_v/2)(C_{out} - C_w) - \frac{\Delta(\varepsilon\rho_{air}W_{out}C_{out})}{\Delta z} \end{aligned} \quad (15)$$

The second term on the RHS of eq. (15) is representative to account for convection. The snag in the CFD model is that the real convection velocity in the z direction in the outlet channel, W_{out} , is not the same as velocity W_s , which is available within Star-CD, because W_s is the net superficial velocity in the porous medium for a channel pair. The term as shown in eq. (15) is coded into a user subroutine in a way that accounts for the velocity gradient in the outlet channel by means of two source

terms and a sink term. In the model, for each computational cell, the source of species in the current cell is the calculated flow from the wall with concentration ($\rho_{\text{air}}C_w$) plus the flow from the upstream cell (zero for the first cell) with concentration ($\rho_{\text{air}}C_{\text{out}}$) for that upstream cell. The sink is the total flow out from the current cell into the downstream cell, which has concentration ($\rho_{\text{air}}C_{\text{out}}$) for the current cell. Formulated in this way the CFD model will solve for the correct species mass fractions, and hence concentrations, in the outlet channel. Caution is needed, however, when interpreting the model output because the velocity and mass flow through the model as a whole relate to the equivalent porous medium and so cannot be used to convert the mass fractions into local species mass flow rates through the wall or along the outlet channel.

OTHER FEATURES OF THE DPF/SCR MODEL

The model also requires details of the pressure loss in the porous medium and the reaction kinetics. These are sourced from the literature and applied as now described.

Pressure Loss in Porous Medium

Equation (16) is derived from geometry and can be used to estimate the soot layer thickness in a square channel both during soot accumulation and during a thermal regeneration.

$$w_p = \frac{1}{2} \left[a - \left[a^2 - \frac{M_p}{N_{\text{cells}} L \rho_p} \right]^{1/2} \right] \quad (16)$$

The equation for a loaded filter as presented by Konstandopoulos et al. [16] is reiterated here as eq. (17) and is used to find the pressure drop across the filter.

$$\Delta p = \frac{\mu Q(a+w_w)^2}{2V_{\text{sub}}} \left[\frac{w_w}{k_o a} + \dots \right. \\ \left. + \frac{1}{2k_{\text{soot}}} \ln \left[\frac{a}{a-2w_p} \right] + \frac{4FL^2}{3(a-2w_p)^4} + \frac{4FL^2}{3a^4} \right] \quad (17)$$

In applying this equation within a DPF monolith CFD model, Q is the global volume flow rate and μ is the local viscosity at the local cell temperature. The second order terms are neglected in this expression.

After the first regeneration, if the regeneration is incomplete, there will be an axial variation in the thickness of the soot layer along the monolith. The model can predict what this will be after a partial or incomplete regeneration, although the model does assume that the soot accumulating at each location at each time step during the regeneration remains constant, which may not be correct, because the wall resistance will not be uniform. However, throughout much of the regeneration the amount of soot accumulating is small compared with the amount being consumed so the prediction will be an

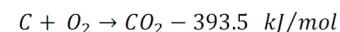
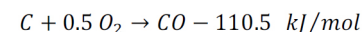
approximation. The effect of the uneven distribution on the wall resistance and hence on the local "through the wall" velocity and on the amount of soot subsequently deposited at each cell location cannot yet be accurately predicted by the current model. If the regeneration is complete, however, the model can continue to model multiple cycles of storage and regeneration.

The final two terms in eq. (17) are for the pressure drop along the inlet and outlet channels. In an SCR that only supports SCR washcoat in the outlet channels, the final term must be modified to make allowance for the smaller outlet channel dimension if the thickness of the washcoat layer is significant.

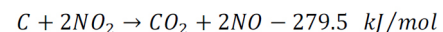
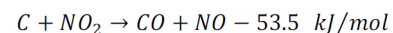
Soot Reactions with Oxygen and with NO_2

The amount of soot particulates entering the domain is expressed as a mass fraction of the gas. The amount of soot deposited the soot cake layer in the filter is also expressed as a mass fraction of the gas. In the earlier paper [10] reaction rate constants attributed to Mogaka et al. were taken from the paper by Awara et al. [17] to determine the reaction rate by combustion of the soot layer. This rate is very slow except during the regeneration, which is initiated by a rise in the exhaust temperature to a value in excess of 850 K. The reaction is exothermic and the effect of the heat released on the solid phase temperature of the porous medium is also accounted for in the model by coding the reaction rate into the enthalpy source term user subroutine. The heat transfer between the gas phase and the solid phase of the analogous porous medium is managed within the current version of Star-CD by supplying the value for $h A_v$ ($\text{W}/\text{m}^3/\text{K}$) via an enthalpy source user subroutine.

Soot combusts with oxygen to both CO and to CO_2 and the reactions are exothermic; net heats of reaction are shown in the equations.

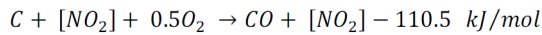
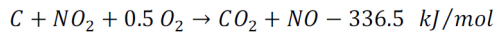


Soot also reacts with NO_2 to produce NO and CO or CO_2 . Again, the reactions are exothermic.



The selectivity of these two NO_2 reactions is such that 16.7% of the carbon reacted is consumed by the first and 83.3 % by the second [12]. A value for activation energy of $43.3 \text{ E}+03 \text{ kJ/kmol}$ is provided by Ahmadinejad et al. [12] but their pre-exponential factor is not stated explicitly. There are other papers that provide kinetic rate constants for soot with NO_2 reactions, for example Shrivastava et al. [18], but their approach is based on the decrease of the diameter of polydispersed soot particles, which may not extrapolate well to the behaviour of a soot cake layer in a DPF. Their activation energy is similar, however, being 47.1 kJ/mol.

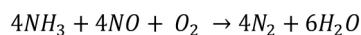
Zouaoui et al. [13] have attempted to resolve this issue specifically for continuously regenerating DPFs. According to [13] there are two further reactions, which they describe as cooperative reactions dependent upon a synergetic effect of O_2 with NO_2 .



They suggest that the activation energy for the soot- NO_2 reaction that produces CO is 66.4 kJ/mol but is only 39.1 kJ/mol for the reaction that produces CO_2 . This is similar to Ahmadinejad et al. [12] if selectivity is taken into account. Their pre-exponential factors are 2440 and 62.2 respectively and there is dependence upon the molar fraction of NO_2 . The paper by Zouaoui et al. [13] gives full details of the activation energies and pre-exponential factors for all six chemical reactions. These six rates have been entered into the porous medium model developed here. Zouaoui et al. [13] provide different rate constants and activation energies for the reactions if water is also present, which will be the case in a real Diesel exhaust, especially if the ammonia for SCR is introduced by an aqueous urea spray. The kinetics, which are used here for model development purposes, however, do not include the effect of water. Tuning of the pre-exponential factors may be necessary when the model is ultimately tested against experimental data.

Kinetic scheme applied for SCR reactions

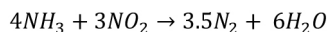
The SCR kinetic scheme published by Olsson et al. [11] is applied here. The standard, fast, and NO_2 SCR reactions and the N_2O production reaction are all included.



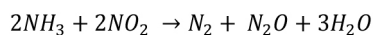
The rate for this standard SCR reaction in mol/mol site/s is $k_4 C_{NO} \theta$.



The rate for this fast SCR reaction in mol/mol site/s is $k_5 C_{NO} C_{NO_2} \theta$.



The rate for this N_2O SCR reaction in mol/mol site/s is $k_6 C_{NO_2} \theta$.



The rate for this N_2O production reaction in mol/mol site/s is $k_7 C_{NO_2} \theta$.

The net ammonia adsorption rate in mol/mol site/s is $k_{1f} C_{NH_3} (1 - \theta) - k_{1b} \theta$. Concentrations C_{NO} , C_{NO_2} and C_{NH_3} are expressed in units of mol/m³ of bulk gas or gas at the catalyst surface. Published values for the parameters of the Olsson et al. scheme [11] are shown in Table 1.

NO oxidation and NH_3 oxidation are also included in the kinetic scheme [11]. Only one ammonia oxidation reaction is included. The scheme was developed for conventional SCR and so this reaction may not be appropriate to completely describe any high temperature ammonia oxidation that occurs during a thermal regeneration of a DPF or SCRF. The NO oxidation rate from [11] includes both forward and backward rates and so should account for the equilibrium shift towards NO if very high temperatures are reached.

Table1. Olsson et al. [11] kinetic parameters applied in current model where k is $A \exp(-E/RT)$, E is activation energy and E_{1b} is $E(1-X\theta)$.

	A (/s)	E (kJ/mol)	Coverage Dependence X
k4	2.3E+08	84.9	-
k5	1.9E+12	85.1	-
k6	1.1E+07	72.3	-
k7	3.6E+04	43.3	-
k1f	0.93	-	-
k1b	1.0E+11	181.5	0.98

Note that the convention used by Olsson et al. [11] makes it necessary to multiply by the stoichiometric coefficient to calculate the correct reaction rate for each participant species.

METHODOLOGY

The parameter values applied in the simulations are listed in Table 2. The model has been run first as a demonstration code with the soot and NO_2 reactions and the soot oxidation reactions all included. In Table 3, the estimated washcoat loading is based on information given by Colombo et al. [4] for an SCRF with both inlet and outlet channels supporting SCR washcoat, but in the model developed here only the outlet channel is washcoated. Other parameters are estimated based on the substrate specifications provided by Schrade et al. [14]. Soot parameter values applied were as in [10].

The input mass fractions of NO , NO_2 and NH_3 were set as 0.000370588, 0.000568235 and 0.00042 respectively for the demonstration runs of the model. The oxygen mass fraction was input as 0.05.

The small mesh used for model development is shown in Fig. 2. The model was run using Star-CD CFD software, version 4.14. The model was run on a single processor of a cluster machine with each node having multiple cpus. Each cpu was operating at 2.6 GHz and had 2GB of RAM. The cases were run as transients with the PISO algorithm. Time steps were 0.05 seconds at maximum and significantly smaller in the parts of the simulation where parameters were changing rapidly.

Table 2. Parameter values used in model development (w/c, washcoat) and in demonstration simulations shown in Figs. 3, 4, 5, 6, 7.

Brick length	150 mm
Brick diameter	116 mm
Mass flow rate	30 g/s
Cell density	300 cpsi
Chan. Dh (non w/c)	1.162 mm
Chan. Dh (SCR w/c)	1.003 mm
DPF porosity (approx.)	63% gas: 37% solid
Wall porosity (approx.)	58% gas: 42% solid
Filtration area, Afilt	1080 m ² /m ³ substrate
Wetted SCR surface	932 m ² /m ³ substrate
Active SCR surface, SA	8440 m ² /m ³ substrate
Wall thickness (bare)	0.305 mm
Wall permeability, ko	9.0E-13 m ²
Soot permeability, ksoot	5.0E-14 m ²
Soot layer density	950 kg/m ³
Soot mass fraction	0.00021
k (substrate),	1.22 W/m/K
ρ (bulk substrate)	540 kg/m ³
ρ (solid substrate)	1448.0 kg/m ³
Cp (substrate)	914 J/kg/K
Vw	0.0464 m ³ pore/m ³ substrate
Capacity, Ω	90 mol sites/m ³ substrate
w/c layer density	1250 kg/m ³
Estimated w/c loading	100 g/litre (outlet chan. only)

The model was ambitious in scope because it models a soot accumulation phase with SCR reactions occurring during that period, followed by a thermal regeneration and finally a further phase of soot accumulation. Currently published SCRF models do not focus on modelling the detail of a thermal regeneration event. The soot accumulation phase was 1050 seconds at 550K, followed by 150 seconds of regeneration at 900 K, followed by a further 550 seconds of soot accumulation at 550K.

The model was also run for a real case when an attempt was made to simulate some data published by Schrade et al., [14]. In that case, although some specific details of the experimental conditions were published, real values for some of the parameters required by the porous medium model were not available so it remained necessary to apply estimated values for some of the parameters. Tuning of the kinetics and other parameters to improve agreement between the model and data has not yet taken place but is planned.

RESULTS OF SIMULATION OF PERFORMANCE OF COMBINED DPF/SCR, INCLUDING REGENERATION

The model runs successfully and some predictions for the demonstration case are shown in Figures 3, 4, 5, 6, 7. Figure 3 shows the temperature at four locations before, during and after the regeneration. The regeneration is initiated by the temperature rising to 900 K but there is a significant exotherm. Figure 4 shows that NO conversion is about 70% except during the regeneration where it falls briefly below 60%. The NO₂ conversion is shown in Figure 5 to be greater than 70% but it falls significantly during the regeneration to about 40%. The NOx slip is quite small in the very early part of the regeneration because the reaction rates are high, and at that stage there is still sufficient ammonia available in storage for reacting with the NOx. This situation is not sustained after 1070 seconds, by which time the brick has heated through and much of the stored ammonia has been released. Figure 6 shows that the ammonia conversion is generally greater than 70 % but falls to about 60% when the stored ammonia is rapidly released in response to the high temperatures reached in the brick. The model, based on Olsson et al. kinetics [11], assumes only one type of site. In consequence, in the model ammonia must be stored and available on a site in order to react. Thus conversion as predicted by the model falls during the regeneration even though ammonia is still being supplied. This is discussed further below.

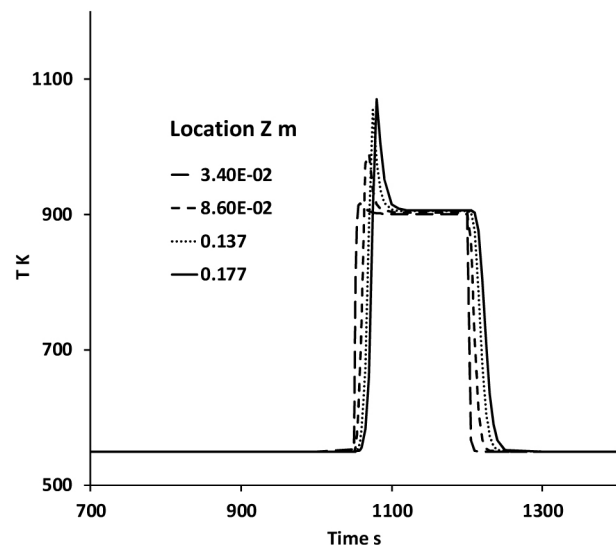


Figure 3. Predicted SCRF temperature during a regeneration.

Figure 7 shows how the soot cake is oxidised and removed during the regeneration. The regeneration starts at 1050 s and proceeds rapidly at the front and in the middle of the brick but by 1080 s, soot remains at the front of the brick whereas at the rear of the brick almost full regeneration has already been achieved. It takes 150 seconds approximately for all the soot to be consumed. The oxygen mass fraction for the simulations was 0.05, which is at the lower end of the range for lean Diesel exhaust. The values shown in Figs. 5, 6, 7 are sensitive to

oxygen concentration. Overall, the simulations suggest that both NO_x and ammonia will slip significantly during a thermal regeneration.

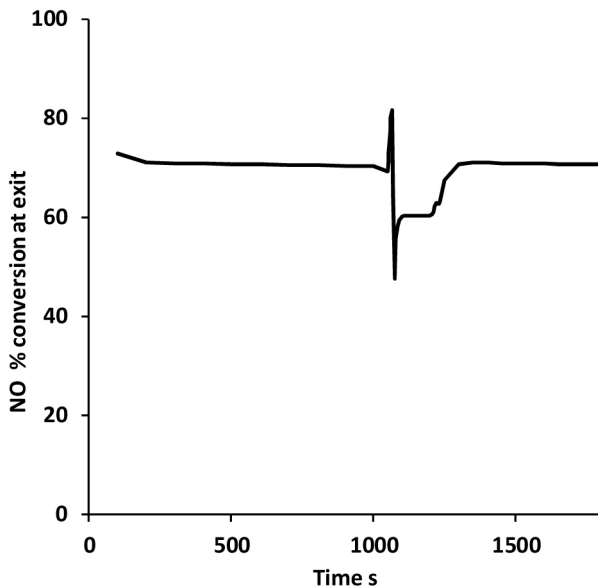


Figure 4. Predicted NO slip from SCRf during a regeneration.

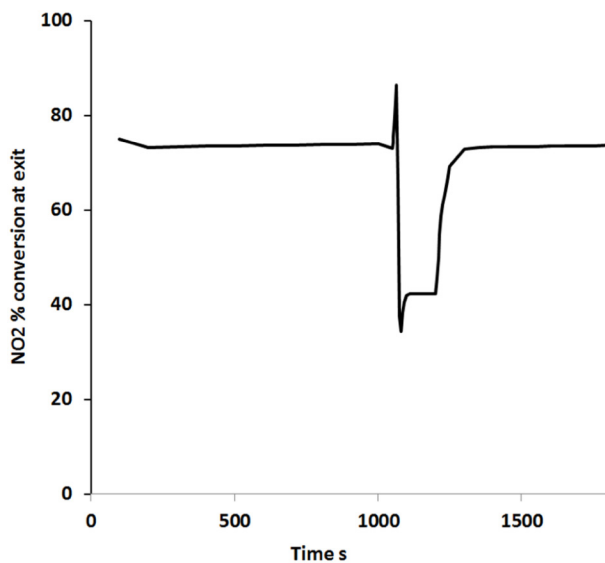


Figure 5. Predicted NO₂ slip from SCRf during a regeneration.

In the case considered here, ammonia is supplied during the thermal regeneration, and both NO_x and ammonia slip are predicted. In a vehicle, dependent upon the control strategy, ammonia might or might not be supplied during a thermal regeneration. A passive regeneration by the NO₂ and soot reaction requires 300 °C or above so an active regeneration is probably required in a passenger car with a cool exhaust. This can be tolerated by some modern zeolites. The model should be capable of predicting for whatever strategy is applied; the simulation output presented here is a demonstration of the model. The model output will obviously change for a different dosing strategy that might be applicable in a real case. The model output would also be subject to change when model parameters, including kinetic constants, are tuned. The model

output presented here may not align with practical experience of conversion rates in an SCRf, but the limitations are with the kinetic scheme and the mass transfer and other parameters currently in use rather than with the modelling approach per se.

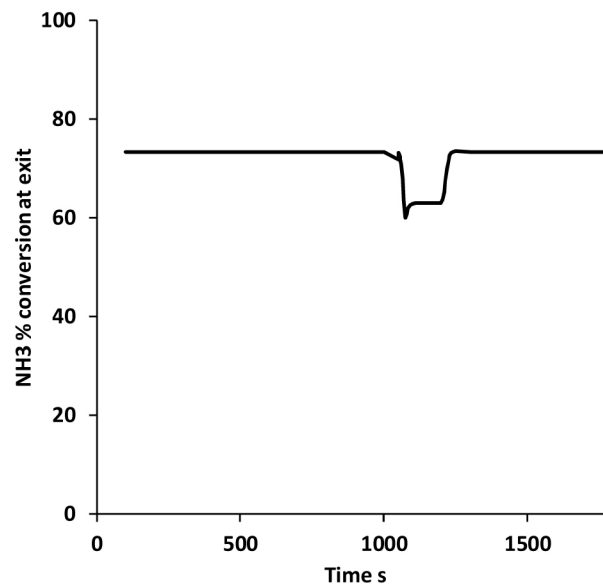


Figure 6. Predicted NH₃ slip from SCRf during a regeneration.

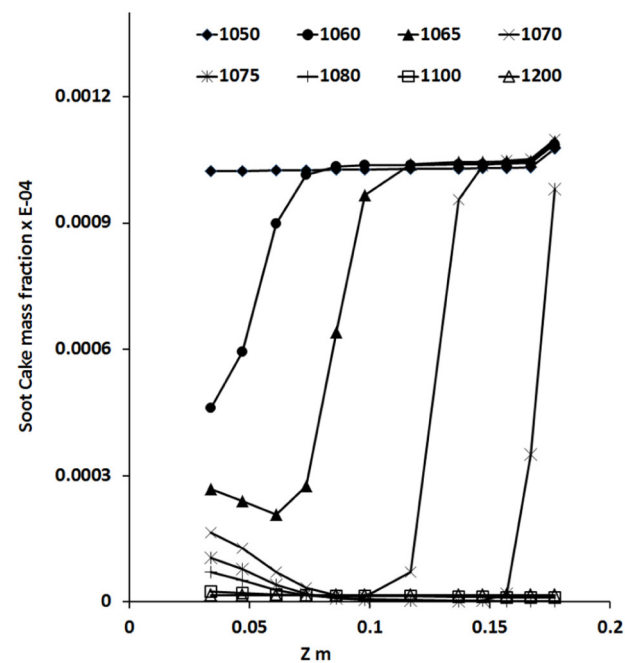


Figure 7. Predicted soot cake mass fraction in SCRf during a regeneration; legend shows time in seconds.

RESULTS FOR MODEL APPLIED TO PUBLISHED DATA

An attempt was made to simulate some of the measured data published by Schrade et al. [14]. They looked at the impact of soot on NO_x conversion and ammonia slip. In their tests the space velocity was 40000 /hour and the temperature was 523 K. The feed gas supplied 250 ppm of ammonia and 200 ppm of NO_x, either all NO, or 50 % of NO₂ or 100% of NO₂. The tests

were run for more than 4000 s and ammonia was supplied between 550 s and 3550 s. The soot loading was either zero or equivalent to 5 grams per litre. The output from the simulations using the current model is shown in Figures 8, 9 and 10.

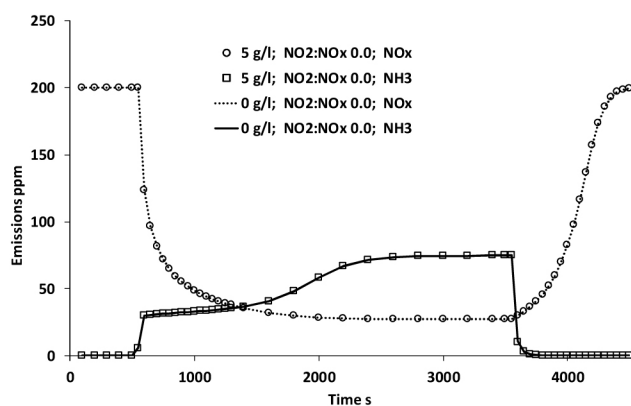


Figure 8. Simulated effect of soot loading on NOx level and ammonia slip for NOx composed of 100 % NO.

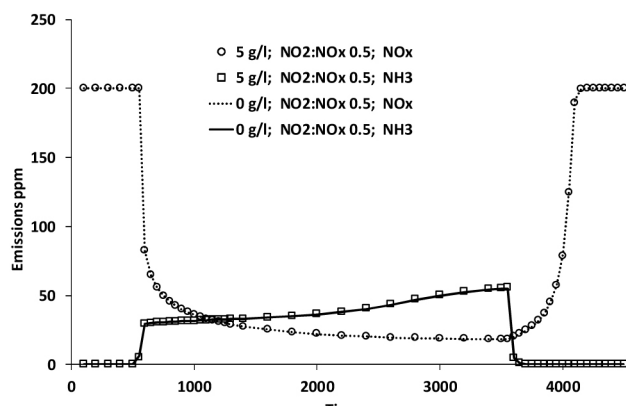


Figure 9. Simulated effect of soot loading on NOx level and ammonia slip for NOx composed of 50 % NO₂ and 50 % NO.

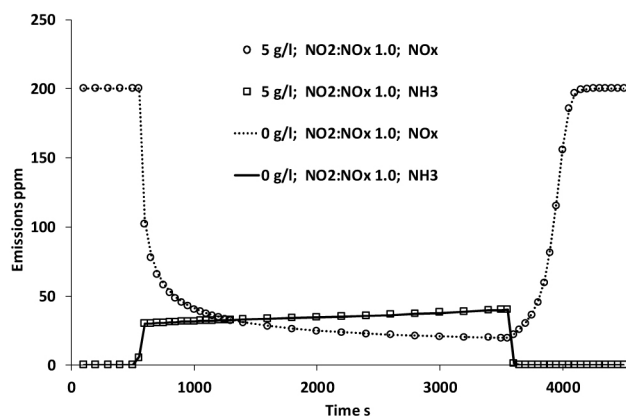


Figure 10. Simulated effect of soot loading on NOx level and ammonia slip for NOx composed of 100 % NO₂.

In Figures 8 and 10 there is negligible effect of soot loading but it is discernible in the ammonia level in Figure 9 for an NO₂ level of 50% of NOx. The simulations show the same trends qualitatively as the experimental data [14] for zero NO₂ and 50% NO₂ in Figures 8 and 9 but not for 100% NO₂ in Figure 10. The data published in [14] show significantly different

behavior for 100% NO₂ and are explained in that paper as the result of inhibition and site blocking effects caused by excess ammonia conditions. Effects of that type are not currently included in the model. Furthermore, the 100% NO₂ condition is not generally encountered, except under laboratory reactor conditions, so the fact that the model described in this paper fails to reproduce this case exactly is of lesser importance.

The published data [14] show almost complete conversion of the NOx during the ammonia dosing phase when NO₂ is zero or 50%, whereas the simulations in Figures 8 and 9 show good but not complete NOx conversion. For reactions between NO₂ and soot, the model contains the recently published kinetics of Zouaoui et al. [13], which should be applicable at the fairly low temperature 523 K in this case. The published data show minimal effect of soot loading under the experimental conditions for NO₂ zero and for NO₂ 50%, so in that respect there is agreement between the simulations and the measurements and the kinetics applied have performed correctly in the model. Comparison of Figures 11 and 12, for the phases without and for the phases with ammonia dosing, shows the effect of soot loading in the model in the presence of NO₂. The differences between Figures 11 and 12 are subtle because the soot and NO₂ reactions are not highly active at 523 K.

The SCR scheme will require tuning to improve the predictions of ammonia slip and NOx conversion. There may also be issues with some of the estimated substrate and catalyst property values applied in the model that relate to the ammonia storage capacity and with the kinetics of ammonia adsorption and desorption. The SCR kinetics applied here were not developed for the catalyst used in [14]. Any effect of soot loading on the ammonia adsorption capacity has also not been included in the model. Ideally, to test the SCR kinetics and the soot/NO₂ kinetics would require extensive experimental investigations on a synthetic gas test bench, similar to [20, 21], but this is outside the remit of this paper, which is focused on a distinctive and novel computational modelling approach for an SCRf.

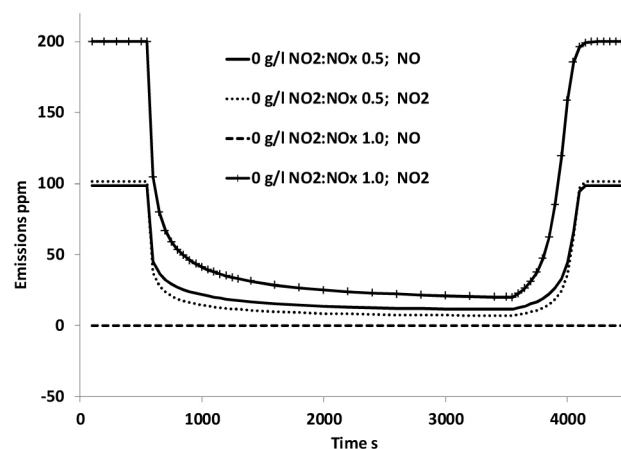


Figure 11. Simulated effect of soot loading on NO and NO₂ levels for 50% and 100% NO₂ with zero soot loading.

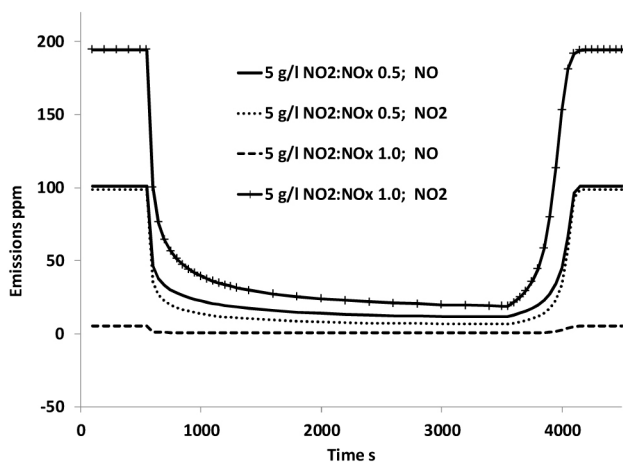


Figure 12. Simulated effect of soot loading on NO and NO₂ levels for 50% NO₂ and 100 % NO₂ with 5 g/litre soot loading.

The Olsson et al. kinetic scheme [11] has only one type of ammonia storage site and ammonia must be stored before it can react. Newer kinetic schemes [20, 21] have two types of site and may provide better descriptions of real data. The current model does not at present encompass all of the many complex possibilities, for example inhibition of SCR reactions by CO and HC in the exhaust stream. The point is that the computational approach offered in this paper can readily accommodate them once good kinetic descriptions are available. When there is a clearer consensus on the strategies to be used in practice with SCRFS, the model can very readily be modified to conform. The point of this paper is to demonstrate the computational approach.

SUMMARY/CONCLUSIONS

The model and its coding are still under development and they are subject to ongoing improvement but the basic framework of the model is now in place. This paper presents the current status of the model. The way that the model output values behave before, during, and after, a thermal regeneration is qualitatively correct. The simulations at 523K and 40k space velocity have also shown some qualitative similarity to the experimental data published in the literature. Some of the model parameters will require tuning before the model can be tested more fully against experimental data. Others need to be replaced with case-specific values for the details of the geometry and the catalyst loading; this is information that is not always available when experimental data is obtained from work published in the literature, and is sometimes confidential. Although at present it is not possible to fully validate the output from the model, nevertheless this study has shown that modelling an SCRFS using the porous medium approach is feasible. The model is simple and is based on numerous assumptions but there is scope for further improvement to the model to provide a realistic description of the performance of an SCRFS. When there is a consensus on regeneration strategies for SCRFS in passenger cars and reliable kinetics are available that are appropriate for those light duty conditions, then the model will be directly applicable.

The nature of this model, based on the porous medium approach, has computational advantages because the number of cells required to describe the SCRFS is relatively small. The model presented in this paper is 1D but could be applied directly to a full 3D model of an SCRFS fitted within a complex exhaust geometry. Economies of scale would be achieved by the use of a coarser computational mesh for the SCRFS than would be required by a detailed channel-scale model or by representative single channel modelling.

REFERENCES

1. Haralampous, O., and Koltsakis, G., "Back-Diffusion Modelling of NO₂ in Catalysed Diesel Particulate Filters", *Ind Eng Chem Res* 43: 875 - 883, 2004
2. Haralampous, O., Koltsakis, G., Samaras, Z., Vogt, C. et al., "Reaction and Diffusion Phenomena in Catalyzed Diesel Particulate Filters," SAE Technical Paper [2004-01-0696](#), 2004, doi:[10.4271/2004-01-0696](#).
3. Tsinoglou, D., Haralampous, O., Koltsakis, G., and Samaras, Z., "Model-based optimization methods of combined DPF+SCR Systems," SAE Technical Paper [2007-24-0098](#), 2007, doi:[10.4271/2007-24-0098](#).
4. Colombo, M., Koltsakis, G., and Koutoufaris, I., "A Modeling Study of Soot and De-NOx Reaction Phenomena in SCRFS Systems," SAE Technical Paper [2011-37-0031](#), 2011, doi:[10.4271/2011-37-0031](#).
5. York, A., Ahmadinejad, M., Watling, T., Walker, A. et al., "Modeling of the Catalyzed Continuously Regenerating Diesel Particulate Filter (CCR-DPF) System: Model Development and Passive Regeneration Studies," SAE Technical Paper [2007-01-0043](#), 2007, doi:[10.4271/2007-01-0043](#).
6. York, A., Watling, T., Ahmadinejad, M., Bergeal, D. et al., "Modeling the Emissions Control Performance of a Catalyzed Diesel Particulate Filter (CDPF) System for Light Duty Diesel Applications," *SAE Int. J. Fuels Lubr.* 2(1):578-589, 2009, doi:[10.4271/2009-01-1266](#).
7. Watling, T., Ravenscroft, M., Avery, G., "Development, validation and application of a model for an SCR catalyst coated Diesel particulate filter", *Catalysis Today* 188 : 32 - 41, 2012
8. Park, S-Y., Rutland, C., Narayanaswamy, K., Schmeig, S., et al., "Development and validation of a model for wall-flow type selective catalytic reduction system", *Proc I Mech E Part D, J Automobile Engineering*, 225: 1641 - 1659, 2011
9. Park, S-Y., and Rutland, C., "Analysis of SCR performance differences caused from flow characteristics of wall flow and flow through type substrate: A simulation study", *Chem Eng Sci*, 88:69-78, 2013
10. Benjamin, S., and Roberts, C., "Three-dimensional modelling of NOx and particulate traps using CFD: A porous medium approach", *Applied Mathematical Modelling*, 31: 2446 - 2460, 2007
11. Olsson, L., Sjoval, H., Blint, R., "A kinetic model for ammonia selective catalytic reduction over Cu-ZSM-5", *Applied catalysis B: Environmental*, 81: 203 - 217, 2008
12. Ahmadinejad, M., Tsolakis, A., Becker, J., Goersmann, C. et al., "Modelling of Soot Oxidation by NO_x in a Diesel Particulate Filter," *SAE Int. J. Fuels Lubr.* 5(1):359-369, 2011, doi:[10.4271/2011-01-2083](#).
13. Zouaoui, N., Labaki, M., Jeguirim, M., "Diesel soot oxidation by nitrogen dioxide, oxygen and water under engine exhaust conditions: Kinetics data related to the reaction mechanism", *Comptes Rendus Chimie*, 17: 672-680, 2014
14. Schrade, F., Brammer, M., Schaeffner, J., Langeheinecke, K. et al., "Physico-Chemical Modeling of an Integrated SCR on DPF (SCR/DPF) System," *SAE Int. J. Engines* 5(3):958-974, 2012, doi:[10.4271/2012-01-1083](#).
15. Hwang, G., Cheng, Y., Ng, M., "Developing laminar flow and heat transfer in a square duct with one walled injection and suction", *Int J Heat and Mass Transfer*, 36 (9): 2429 - 2440, 1993
16. Konstandopoulos, A., Kostoglou, M., Skaperdas, E., Papaioannou, E. et al., "Fundamental Studies of Diesel Particulate Filters: Transient Loading, Regeneration and Aging," SAE Technical Paper [2000-01-1016](#), 2000, doi:[10.4271/2000-01-1016](#).

17. Awara, A., Opris, C., and Johnson, J., "A Theoretical and Experimental Study of the Regeneration Process in a Silicon Carbide Particulate Trap Using a Copper Fuel Additive," SAE Technical Paper 970188, 1997, doi:10.4271/970188.
18. Shrivastava, M., Nguyen, A., Zheng, Z., Wu, H-W., et al., "Kinetics of Soot Oxidation by NO₂", *Environ Sci Technol*, 44: 4796 - 4801, 2010
19. Dwivedi, P., and Upadhyay, S., "Particle-Fluid Mass Transfer in Fixed and Fluidized Beds", *Ind Eng Chem Process Des Dev*, 16(2):157 - 165, 1977
20. Song, X., Parker, G., Johnson, J., Naber, J. et al., "A Modeling Study of SCR Reaction Kinetics from Reactor Experiments," SAE Technical Paper 2013-01-1576, 2013, doi:10.4271/2013-01-1576.
21. Song, X., Naber, J., Johnson, J., and Parker, G., "An Experimental and Modeling Study of Reaction Kinetics for a Cu-Zeolite SCR Catalyst Based on Engine Experiments," SAE Technical Paper 2013-01-1054, 2013, doi:10.4271/2013-01-1054.

CONTACT INFORMATION

Prof. S. F. Benjamin
Automotive Engineering Applied Research Group
Faculty of Engineering and Computing
Coventry University, UK.
s.benjamin@coventry.ac.uk

DEFINITIONS/ABBREVIATIONS

a - channel dimension, side length if square cross section (m)
A_{fit} - filtration area per unit monolith volume (m²/m³)
A_v - wetted surface area per unit monolith volume (m²/m³)
A_{wall} - superficial area of wall (m²)
C - mass fraction
C_g - species mass fraction in the gas phase
C_w - species mass fraction in flow emerging from SCR layer on porous wall
C_{out} - species mass fraction in flow in the outlet channel
C_{pore} - species mass fraction in pores in SCR washcoat
C_{ps} - species mass fraction post soot, i.e. after the soot layer, before the SCR layer
C_{NO} - concentration of NO (mol/m³)
C_{NO2} - concentration of NO₂ (mol/m³)
C_{NH3} - concentration of NH₃ (mol/m³)
D - species diffusivity (m²/s)
d_p - diameter of wall pore (m)
E_p - activation energy of reaction with soot particulate (kJ/kmol)
F - constant, 28.454 for square channels
h - heat transfer coefficient (W/m²/K)
k_o - specific permeability (m²) of pristine channel wall
k_{soot} - specific permeability (m²) of soot particulate layer
K_{mi} - mass transfer coefficient (m/s)
k_p - frequency factor for reaction with soot particulate (/s)
k_k - frequency factor for reaction with soot particulate (mol/kg soot/s)
K_{pore} - mass transfer coefficient inside washcoat layer (m/s)
L - channel length, monolith length (m)

M_i - molecular mass of species i (kg/mol)
M_p - accumulated mass of particulate matter or soot (kg)
M' - total mass flow rate through DPF or SCR monolith (kg/s)
M_{wall} - mass flow rate through superficial area A_{wall} (kg/s)
N_{cells} - number of cells (channels) containing soot
Δp - pressure drop (Pa)
Q - volume flow rate (m³/s)
R - gas constant, 8.314 (J/(mol K))
RANS - Reynolds averaged Navier-Stokes
RR - reaction rate (/s)
R_i - net rate of production of species i by reaction (mol /s /m³ reactor)
SRR - rate of reactions with soot kg/s/m³
S_A - wetted active area in the pores in the SCR washcoat layer (m²/m³)
t - time (s)
T - temperature (K)
U - velocity in substrate channel (m/s)
U_s - superficial velocity for the porous medium, ε U (m/s)
V - velocity in y direction (m/s)
V_{sub} - overall volume of monolith DPF-SCR or SCR (m³)
V_w - volume in solid phase (pore volume) per unit volume of reactor (m³/m³ reactor)
V_{wall} - superficial velocity through the filter wall (m/s)
w_p - particulate layer thickness that has accumulated on filter wall (m)
w_w - monolith wall thickness (m)
W - velocity in z direction (m/s)
W_s - superficial velocity in bulk porous medium model, εW_{channel} (m/s)
W_{out} - velocity in the outlet channel (m/s)
y - flow direction through the wall
z - axial coordinate
ε - porosity of bulk monolith expressed as a void fraction
ε_p - porosity of SCR washcoat layer expressed as a void fraction
μ - viscosity (kg/(m s))
μ_t - turbulent dynamic viscosity (kg/(m s))
ρ - density (kg/m³)
ρ_{air} - density of air/exhaust (kg/m³)
ρ_p - density (kg/m³) of layer of particulate matter or soot
σ_s - turbulent Schmidt number
Ω - ammonia storage capacity parameter (mol-sites /m³ reactor)
θ - fraction of sites occupied by ammonia

APPENDIX

APPENDIX A - MASS TRANSFER IN THE POROUS WALL OR WASHCOAT LAYER

Park et al. [8] suggest that the mass transfer coefficient expression obtained from a paper by Dwivedi et al. [19], which is dependent upon Reynolds number, can be applied to model diffusion inside the porous wall or washcoat layer. The expression is

$$K_{pore}(m/s) = \frac{V_{wall}}{\varepsilon_p S_C^{2/3}} \left[\frac{0.765}{Re^{0.82}} + \frac{0.365}{Re^{0.386}} \right] \quad (A1)$$

V_{wall} is $M_{wall} / (\rho A_{wall})$ and ε_p is the void fraction of the porous wall or washcoat layer. The Schmidt number is found from $\mu / (\rho D_m)$.

From Park et al. [8] the mass transfer is

$$K_{pore} S_A \rho (C_w - C_{pore}) \quad kg \ s^{-1} m^{-3}$$

So it is necessary to know the active surface area in the pores, S_A . Park et al. [8] use the expression

$$S_A = 6 (1 - \varepsilon_p) / d_p \quad (A2)$$

Equation (A2) is the standard expression for packed bed of spheres with active surfaces.

The porosity of the porous wall or washcoat layer, ε_p is likely to be in the range 0.5 to 0.65. The pore size d_p is stated in [4] to be 20 microns and in [14] to be 22 microns. Thus an estimate for S_A would be 120,000 m^2/m^3 washcoat. This is a very high value and may not be appropriate for an SCR washcoat layer, where the porous structure is better described as a bundle of tortuous capillaries, rather than the void space between spheres. S_A should increase with an increase in porosity, i.e. when there are more capillaries per unit of wall entry-face area. But according to eq. (A2) S_A will decrease as the porosity increases. Thus eq. (A2) is not correct when the porous wall is considered as multiple capillaries rather than as packed spheres. A better expression is eq. (A3). Equations (A2) and (A3) give the same value for S_A when the porosity is 0.6. This has enabled the erroneous use of eq. (A2) for walls or washcoat layers with porosities near 0.6, which fortuitously lies in the range of typical values. The preferred expression is eq. (A3).

$$S_A = 4 \varepsilon_p / d_p \quad (A3)$$

The value 105,455 m^2/m^3 washcoat is estimated from eq. (A3) for 22 micron capillaries and 58 % porosity. If the SCR washcoat loading is in the region of 0.08 m^3 washcoat/ m^3 substrate, then the value for S_A is 8436 but expressed in units m^2/m^3 substrate. This value for S_A has been used for model development purposes to produce the results reported in this paper.

APPENDIX B - SPECIES DEFINED IN THE COMBINED SCR/DPF CFD MODEL

Table B1. Species defined in the combined SCR/DPF CFD model. Values for D and σ_s in this table are for species in the fluid; see the footnote after the table for values of D and σ_s for all species in the porous medium.

	Soot transported in gas phase	NO, O ₂ , NO ₂ and NH ₃ in inlet channel and in bulk gas	Soot deposited in cake layer #
Effective eq.	(2)	(4)	(2)
Source term	Included	NOT included	Included
Transient term	Included	Included	Included
Convective term	Included	Included	NOT included
Diffusion flux term	Included in fluid	Included in fluid	Suppressed
In fluid Diffusivity, D	1E-06	8.0E-05 (NO) 6.3E-05 (NO ₂) 7.6E-05 (NH ₃) 6.9E-05 (O ₂)	1E-28
In fluid Turb Schmidt σ_s	0.9	0.9	5E+28
Initial conc. in porous medium	0.0002	0.0001	0.0000005

Table B1 (cont). Species defined in the combined SCR/DPF CFD model. Values for D and σ_s in this table are for species in the fluid; see the footnote after the table for values of D and σ_s for all species in the porous medium.

	NO, O ₂ and NO ₂ post the soot layer #	NO, O ₂ , NO ₂ and NH ₃ in pore in SCR w/c layer #	Adsorbed ammonia # θ
Effective eq.	(5)	(12)	(14)
Source term	Included	Included	Included
Transient term	Included	Included	Included
Convective term	NOT included	NOT included	NOT included
Diffusion flux term	Suppressed	Suppressed	Suppressed
In fluid Diffusivity, D	1E-28	1E-28	1E-28
In fluid Turb Schmidt σ_s	5E+28	5E+28	5E+28
Initial conc. in porous medium	0.000002	0.000002	0.0001

	NO, O ₂ , NO ₂ and NH ₃ post the SCR w/c layer, leaving the wall #	NO, O ₂ , NO ₂ and NH ₃ in the outlet channel #
Effective eq.	(10)	(15)
Source term	Included	Included (& takes a/c of convection)
Transient term	Included	Included
Convective term	NOT included	NOT included
Diffusion flux term	Suppressed	Suppressed
In fluid Diffusivity, D	1E-28	1E-28
In fluid Turb Schmidt σ_s	5E+28	5E+28
Initial conc. in porous medium	0.000002	0.000002

Footnotes to Table B1

[1] # Species marked # have values only in the porous medium cells in the model, not in the fluid cells. Values applied for D and σ_s suppress diffusion in the fluid.

[2] For ALL species in this table, the diffusivity in the porous medium is assigned the value 1E-28 and the turbulent Schmidt No. is assigned the value 1E+28. This suppresses diffusion in the porous medium in all cases. The diffusivity values in this table refer to transport in the fluid, e.g. in the duct prior to the porous medium. Where there is diffusion in the porous medium that is accounted for in the model, it is dealt with by source terms as described in the main body of this paper.